iJRASET
International Journal For Research in Applied Science and Engineering Technology

INTERNATIONAL JOURNAL FOR RESEARCH

IN APPLIED SCIENCE & ENGINEERING TECHNOLOGY

Volume: 9 **Issue:** XII **Month of publication:** December 2021

DOI: https://doi.org/10.22214/ijraset.2021.39684

www.ijraset.com

Call: 08813907089 | E-mail ID: ijraset@gmail.com

International Journal for Research in Applied Science & Engineering Technology (IJRASET)
ISSN: 2321-9653; IC Value: 45.98; SJ Impact Factor: 7.538
Volume 9 Issue XII Dec 2021- Available at www.ijraset.com

Novel Control Approach with FRT capability for Grid connected HYBRID distributed generation system using ANN controller based DVR

Ashok Babu Valluri[1], Dr. Kotni Sri Kumar[2]
[1, 2]*Department of Electrical & Electronics Engineering, University College of Engineering (A), JNTU Kakinada, India*

Abstract: ***For ever increasing power demand and depletion of conventional energy resources, Renewable Energy Systems (RES) became an alternative source of electricity to reduce the load stress on the Power Grid. Although several control & design modifications are presented in past literature to improve reliability & performance of through Distribution Generation (DG) technologies, they always fall short in some aspects of voltage stability and Fault Ride Through (FRT) capabilities. The main aim of the project is Protecting Critical load from Grid side altercations which occur due to harmonics generated by DG's and Short circuit faults near to load center. This project proposes the application of a Dynamic Voltage Restorer (DVR) to enhance the power quality and improve the Fault Ride Through (FRT) capability of a three-phase medium-voltage network connected to a hybrid distribution generation (DG) system. In this hybrid farm, the Photo Voltaic (PV) plant via single-stage energy conversion (DC-AC inverter) & DFIG (Doubly-Fed Induction Generator) based Wind power plant are connected to the same Point of Common Coupling (PCC). For MPPT of wind power plant, we use Pitch Angle Control (PAC) technique. This topology allows Perturb and observe (P&O) based MPPT algorithm for PV plant through connection of the DG (Distribution generation) system to the public grid through a step-up transformer. In addition, the DVR based on Artificial Neural Network (ANN) controller is connected to the same PCC. Different fault condition scenarios are tested for improving the efficiency and the quality of the power supply and compliance with the requirements of the sensitive Load. The efficiency of this control technique is that it enhances restoration and harmonics suppression capabilities of DVR which are far superior than that of PI controller used in existing model.***

Keywords: RES, DG, LVRT, FRT, PV, DFIG, PCC, MPPT, P&O, DVR, PI, ANN, THD, Voltage stability.

I. INTRODUCTION

Renewable energy is obtained from natural resources that refill in less than a human lifetime without diminishing the planet's resources. These resources, such as sunshine, wind, rain, tides, waves, biomass, and thermal energy stored in the earth's crust, have the advantage of being practically everywhere available in one form or another. They're practically indestructible. What's more, they don't have much of an impact on the climate or the ecosystem. On the other hand, fossil fuels such as oil, coal, and natural gas are only accessible in finite amounts. They will eventually run out if we continue to remove them. Despite the fact that they are created naturally, they do not replenish as rapidly as we humans consume them. Today, the world continues to rely significantly on fossil fuels, even subsidising them. Meanwhile, the pollution they produce has hit new highs, ranging from climate-damaging greenhouse gases to health-endangering particulates. And when anything goes awry, such as when the Deepwater Horizon oil platform exploded in 2010, the ramifications are devastating. Renewable energy has grown at a higher rate than all other energy sources since 2011. Renewable energy experienced another record-breaking year in 2020, with installed power capacity increasing by more than 256 gigawatts (GW) — the most ever. Renewable energy already accounts for more than 29% of our power, and this number is steadily increasing. Many rural settlements across the world are unable to connect to an electric power system, either physically or monetarily. Small isolated diesel generators are used to provide the electrical demand in these locations. Due to reduced fossil fuel costs and challenges in fuel transportation and generator maintenance, the operational costs connected with these diesel generators may be excessively high. Renewables are the most cost-effective source of new power production technology in many regions of the world, and costs are continuing to fall. Renewable energy is the sole method to increase energy access to all residents, particularly those living in urban slums and informal settlements, as well as those living in suburban and peri-urban regions, especially in emerging cities. Renewable energy sources, such as solar photovoltaic (PV) and wind turbine generators, offer a viable alternative to engine-driven generators for power generation in off-grid communities in such circumstances. In many off-grid circumstances, hybrid energy systems have been shown to drastically cut the entire life cycle cost of independent power supplies while still delivering a dependable supply of electricity utilising a combination of energy sources.

Many hybrid systems have been deployed across the world, and the growing renewable energy sector has now produced dependable and cost-effective systems based on a range of technologies. India's total renewable energy potential (up to 2032) is expected to be 220 GW, according to our research.

Power quality is an umbrella term that refers to a wide range of electromagnetic phenomena that describe voltage and current at a certain time and location on the power system. Electromagnetic disturbances can be caused by the increased usage of electronic equipment as a result of the increased use of DG connections at the distribution system level. Harmonics, inter harmonics, interruptions, flicker, voltage imbalances, and voltage sag are examples of low-frequency, short-duration processes that cause electromagnetic disturbances. Voltage sag is a short-term phenomenon in which the rms voltage drops to between 0.1 and 0.9 pu for periods ranging from 0.5 to 1 minute. Voltage sag propagates across the electrical system, impacting loads and utility equipment despite its brief duration. Voltage sags are frequently linked to system failures. Switching high loads or starting large motors can also cause it. In today's automated industry, voltage sag is the most prevalent cause of equipment failure, resulting in considerable financial losses. As a result, it is critical to prevent the repercussions of voltage sag and to address the problem in a cost-effective manner. Voltage disturbances can be attenuated by the DVR. It is often positioned in the distribution system between the load and the source to provide quick voltage support by injecting the required voltage in series with the mains voltage via an injection transformer. When the network is connected to a hybrid distributed generation system, this paper presents a simulation analysis to show how the DVR can attenuate voltage disturbances, reduce their impact on overall industrial load stability, and increase FRT capabilities. Under various fault scenarios such as short circuits and voltage sags, a DVR based on Artificial Neural Network (ANN) controller technique is created and assessed.

II. MATHEMTICAL MODELLING AND SYSTEM DESCRIPTION

PV and wind energy technologies, in particular, have improved their integration in hybrid power system setups. This combination is one of the most efficient designs, and it may be utilised in both grid-connected and freestanding modes. Because solar and wind energy are complementary in nature, they can be combined to solve the problem of intermittency and supply more stable, high-quality power to the grid and remote places. PV-wind hybrid systems have been the subject of various research projects in recent years. This study compiles a number of research papers on PV-wind hybrid power systems from the literature. Several research suggested combining PV with DFIG-based wind generation in a hybrid design to provide sustainable electricity to remote load centres. Simple design, decoupled control of active and reactive powers, partially rated converters, and maximum wind energy extraction from the turbine are only a few of the advantages of this configuration.

In Fig 1, the proposed topology is depicted. It comprises of a 106.5kW PV plant with a three phase PWM inverter, three phase AC throttle filter, and a step-up transformer that is coupled to a distribution system. The DFIG has a nominal output power of 151 kW and supplies the load by connecting to the grid via a step-up transformer at the PCC. As a result, the hybrid system's overall power output is predicted to be 257.5MW.

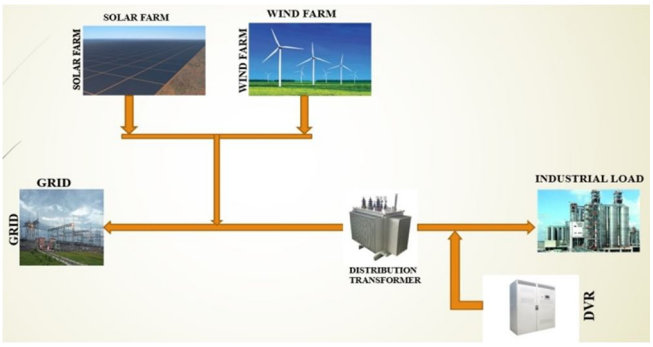

Fig (1): Hybrid generation system with DVR and a load connected to grid.

The following are the simulation scenarios provided in this paper:

1) The DVR is turned off and no fault is applied.
2) The DVR is also turned off, but the fault is applied.
3) The same scenarios as before, but with the DVR turned on.

A. Photovoltaic Power Plant

PV plant array consist of 25 series modules and 20 parallel strings (type: Solar module -1Soltech 1STH-215P).

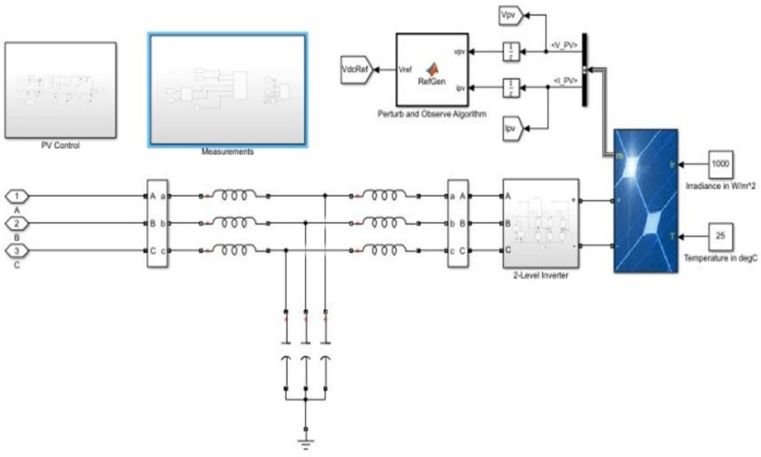

Fig (2): PV farm 106.5KW connected to grid via inverter related to 106.5KVA- 415/11KV transformer

1) Mathematical Equivalent Circuit for Photovoltaic Array

Fig 3 depicts the equivalent circuit of a PV cell. The cell photocurrent is represented by the current source Iph. The intrinsic shunt and series resistances of the cell are Rsh and Rs, respectively. Because the value of Rsh is usually very large and the value of Rs is usually very tiny, they can be ignored to simplify the study. PV cells are grouped into bigger units called PV modules, which are then connected in series or parallel to form PV arrays which generate energy in PV generation systems.

The mathematical analysis of a PV array is provided as Module photo-current (Iph):

$$Iph = [Isc + Ki(T - 298)] \times \frac{Ir}{1000} \quad (1)$$

Here, Iph: photo-current (A); Isc: short circuit current (A) ; Ki: short-circuit current of cell at 25 °C and 1000 W/m2; T: operating temperature (K); Ir: solar irradiation (W/m2).

The module reverse saturation current I_{rs} is derived as follows:

$$Irs = \frac{Isc}{\left[\exp\left(\frac{qVOC}{NSknT}\right) - 1\right]} \quad (2)$$

Here, q: electron charge, = 1.6 × 10−19C; Voc: open circuit voltage (V); Ns: number of cells connected in series; n: the ideality factor of the diode; k: Boltzmann's constant, = 1.3805 × 10−23 J/K.

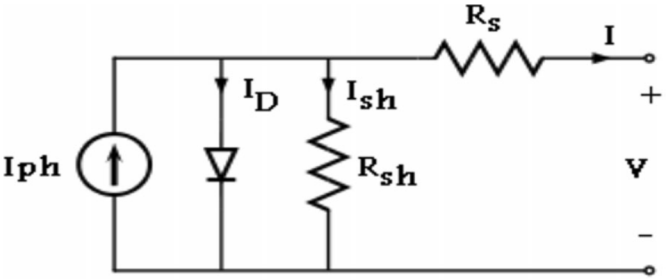

Fig (3): PV cell Equivalent circuit diagram

The module saturation current I0 varies with the cell temperature, which is given by:

$$Io = Irs.\left(\frac{T}{Tr}\right)^3 .\exp\left[q.Eg0.\frac{\left\{\frac{1}{T} - \frac{1}{Tr}\right\}}{n}.K\right] \quad (3)$$

Here, Tr = nominal temperature = 298.15 K & Eg0 = band gap energy of the semiconductor, = 1.1 eV;

The final current output of PV module is:

$$I = Np.Iph - Np.Io\left[\exp\left(\frac{\frac{V}{Ns}+I.\frac{Rs}{Np}}{n}.Vt\right)-1\right] (4) - Ish$$

Where; $Vt = \frac{KT}{q}$ & $Ish = \frac{\left[V.\left(\frac{Np}{Ns}\right)+I.Rs\right]}{Rsh}$

.

Here: Np: number of PV modules connected in parallel; Rs: series resistance (Ω); Rsh: shunt resistance (Ω); Vt: diode thermal voltage (V).

The maximum power point tracker (MPPT) is used to control photovoltaic power conversion. MPPT provides for high efficiency power transfer and is dependent on both solar irradiation and the electrical characteristics of the load.

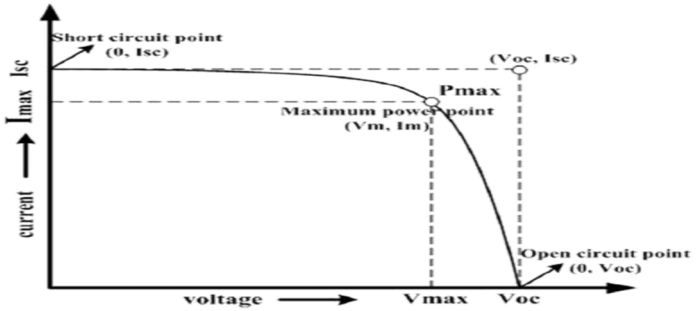

Fig (4): I-V characteristics of PV cell

Under varying conditions, such as changing solar irradiance, temperature, and load, maximum power point tracking (MPPT) is an algorithm implemented in photovoltaic (PV) inverters to continuously adjust the impedance seen by the solar array to keep the PV system operating at, or close to, the peak power point of the PV panel.

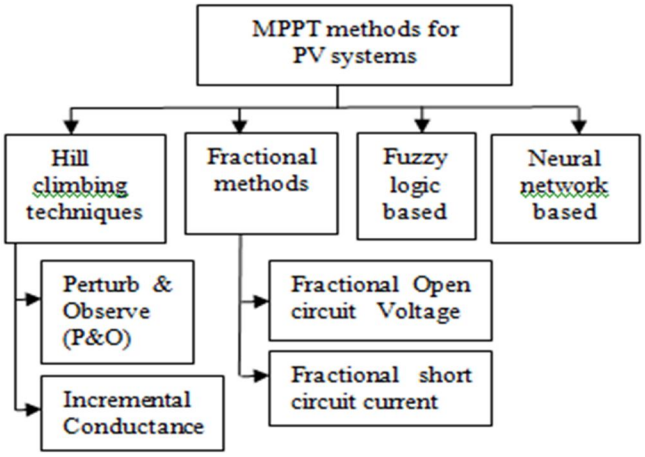

Fig (5): Classification of MPPT algorithms

Among the methods presented in Fig (5), the perturb and observe (P&O) algorithm is used in the project paper. This is one of the most commonly utilized traditional methods. The traditional P&O algorithm works by perturbing the PV voltage (Vpv) and observing the variation of PV power (P_{pv}); if an increase in voltage results in an increase in power, this indicates convergence to the maximum power zone; if the power decreases, the voltage must be reduced to coincide with the MPP. Figure 7 shows the P&O flowchart, where d is the duty cycle of the single stage converter and d is the duty cycle variation. The new P&O algorithm is based on a P_{pv} vs. P_{mpp} comparison. The V_{pv} is then lowered or increased to match the MPP. The V_{pv} is then lowered or increased to match the MPP.

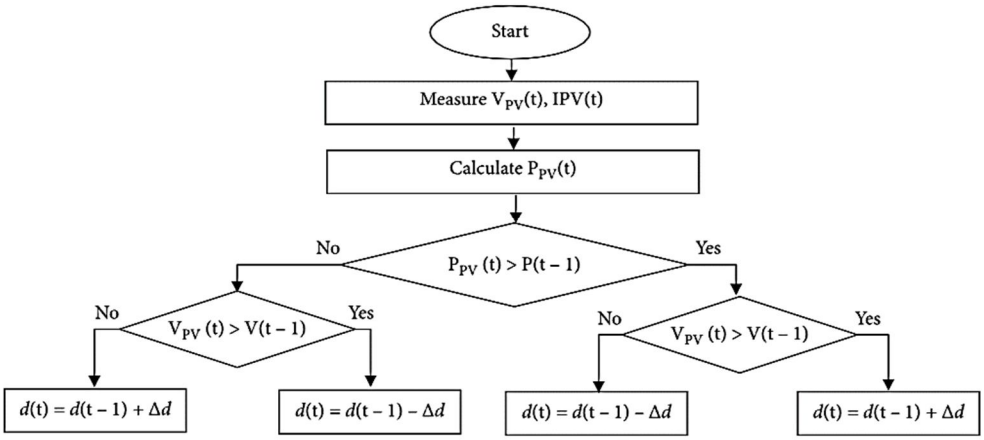

Fig (6): Flowchart of the P&O algorithm

The Two-level Voltage source inverter topology is presented in fig 7,

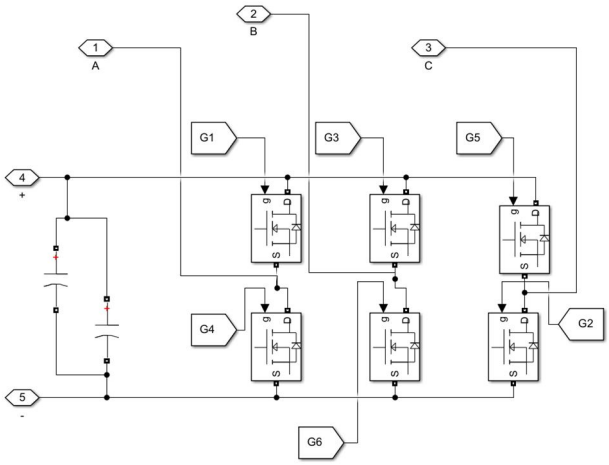

Fig (7): Two level inverter Topology

The Vdc output voltage is set at 725V, and the IGBT 2-level inverter converts DC power from a 725 Vdc source to 415 Vac, 50 Hz, using the PWM approach. The grid is connected to the inverter via an inductive and capacitive grid filter, as well as a low frequency transformer that steps up the voltage from 0.415 kV to 11 kV to reduce losses and filter out harmonic frequencies when PV energy is delivered to the grid.

B. DFIG Based Wind Power Plant

The wind turbine captures the kinetic energy of the wind and converts it to mechanical power Pm. The wind power plant consists of a single DFIG-based wind turbine with a 575 Vac output voltage that produces 150 KW. The DFIG (double-fed induction generator) is a common generating principle in wind turbines.

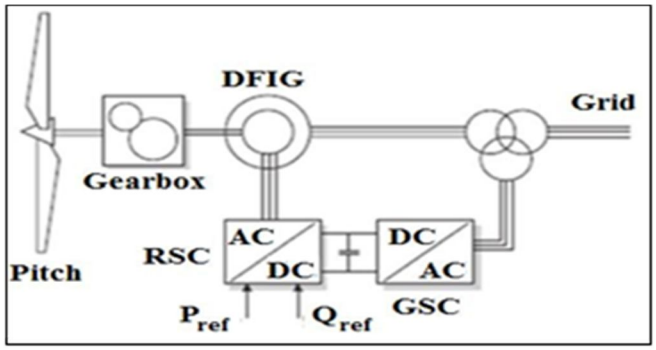

Fig (8): Aerodynamic modeling of the DFIG WindTurbine

As illustrated in fig 8, it is based on an induction generator with a multiphase wound rotor and a multiphase slip ring assembly with brushes providing access to the rotor windings. The stator windings are connected to the grid, while the rotor windings are connected to the converter through slip rings and a back-to-back voltage source converter that regulates both the rotor and grid currents. As a result, the rotor frequency can vary freely from the grid frequency (50 Hz). It is feasible to modify the active and reactive power provided to the grid from the stator regardless of the generator's turning speed by employing the converter to manage the rotor currents. The proposed system's mathematical modelling, includes subsystems such as the wind turbin87e, two mass drive train models, DFIG, Grid linked transmission line, RSC, and GSC. The comprehensive mathematical modelling of each component will be explained in the next section.

1) Modelling of Wind Turbine

Wind turbine model is developed with the help of following power equations as:

$$Tw = \frac{1}{2} \cdot \frac{(\rho \cdot V\omega^3 \cdot R \cdot C_p)}{\omega r} \quad (5)$$

$$\lambda_i = R\frac{C_f}{\lambda} \quad (6)$$

$$C_p = \frac{1}{2} \cdot (0.22\beta - \lambda i - 2) \cdot e^{\lambda i} \quad (7)$$

Where, Tw= wind turbine torque, ρ= air density, Vw= wind velocity R=Radius of the blade, C_p=Power coefficient, λi=Tip-speed ratio, β=Pitch angle.

2) Modelling of DFIG

The voltages and currents of the stator and rotor are transferred to the dq frame for analysis. The DFIG voltage equations[11], the differential equations (8) to (15) are derived,

$$\frac{dI_{dr}}{dt} = V_{dr} - R_r I_{dr} + S\omega_s \lambda_{qr} - \frac{X_m}{X_r}\frac{d}{dt} i_{ds} \quad (8)$$

$$\frac{dI_{qr}}{dt} = V_{qr} - R_r I_{qr} - S\omega_s \lambda_{dr} - \frac{X_m}{X_r}\frac{d}{dt} i_{qs} \quad (9)$$

$$\frac{dI_{ds}}{dt} = V_{ds} - R_s I_{ds} - \omega_s \lambda_{qs} - \frac{X_m}{X_s}\frac{d}{dt} i_{dr} \quad (10)$$

$$\frac{dI_{qs}}{dt} = V_{qs} - R_s I_{qs} + \omega_s \lambda_{ds} - \frac{X_m}{X_s}\frac{d}{dt} i_{qr} \quad (11)$$

Where,

$$\lambda_{ds} = X_s i_{ds} + X_m i_{dr} \quad (12)$$

$$\lambda_{qs} = X_s i_{qs} + X_m i_{qr} \quad (13)$$

$$\lambda_{dr} = X_r i_{dr} + X_m i_{ds} \quad (14)$$

$$\lambda_{qr} = X_r i_{qr} + X_m i_{qs} \quad (15)$$

Two pulse width modulation inverters are connected back to back through a dc connection in the DFIG converter type. The RSC injects a slip frequency AC voltage into the rotor, whereas the GSC injects a power frequency AC voltage into the grid and vice versa. It keeps the voltage on the dc connection constant. In this study, the RSC and GSC controllers are not discussed. In the future, RSC and GSC control can be added to this model for stability investigations.

The following is the power balance equation for the converter model:

$$P\ RSC = P\ GSC + P\ dc \quad (16)$$

$$P\ RSC = Vdr\ idr + Vqr\ iqr \quad (17)$$

$$P\ GSC = Vdg\ idg + Vqg\ iqg \quad (18)$$

$$P\ dc = CVdc\ dVdc/dt \quad (19)$$

Where, PRSC, PGSC, Pdc are powers at RSC, GSC side and DC link. Vdg, Vqg , Idg, Iqg are AC voltage at GSC side in dq frame, Vdc – DC link voltage, C- DC link capacitor value.

In recent years, pitch variable-speed wind turbines have become the most popular. For variable-speed wind turbines, there are commonly two control techniques. When the wind speed is below a rated value, the speed controller may continuously modify the rotor speed to keep it at a level that delivers the highest power coefficient, increasing the turbine's efficiency.

When the rotating speed is kept constant and the wind speed exceeds the rated wind speed, pitch angle control is necessary. The power output can be affected by small variations in pitch angle.

The purpose of the control may be summed up in three objectives:

a) When the wind speed is less than the rated wind speed, the power output is optimised.
b) When the wind speed exceeds the rated wind speed, keep the rotor power at design limits.
c) Reduce the fatigue stresses on the mechanical components of the turbine.

C. DVR Topology

The DVR injects a three-phase AC voltage that is coordinated with the AC system's distribution feeder voltage. To manage the bi-directional interchange of active and reactive power between the DVR and the AC system, the injected voltage amplitude and phase may be changed. The DVR's primary function is to balance and control voltages while also preventing harmonics from the source voltage from reaching the load.

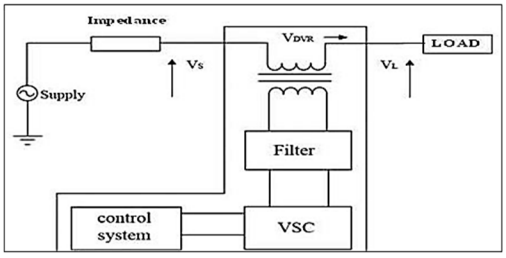

Fig (9): Equivalent circuit diagram of DVR

The basic structure of the DVR shown in Fig. 9 consists of:

1) Injection transformer
2) Harmonic filter
3) Energy storage device
4) VSC
5) DC charging circuit
6) Control system.

The following is the series voltage injected by the DVR:

VDVR= VL+ZTHIL-VTH (20)

Where, VL=load voltage, ZTH=load impedance , IL= load current and VTH=System voltage during the fault.

The load current IL is calculated as follows:

$$I_L = \frac{PL+jQL}{V} \quad (21)$$

The equation may be rewritten as follows, using VLas a reference:

$$V*DVR=VL\angle 0+ZTH\angle(\beta-\theta)-VTH\angle\delta \quad (22)$$

with θ=tan−1($\theta L/PL$)

The DVR's complicated power output may be expressed as:

$$S\ DVR=VDVRI*DVR \quad (23)$$

D. ANN Based DVR Controller Design

The Fig (10) represents the general model of ANN followed by its processing,

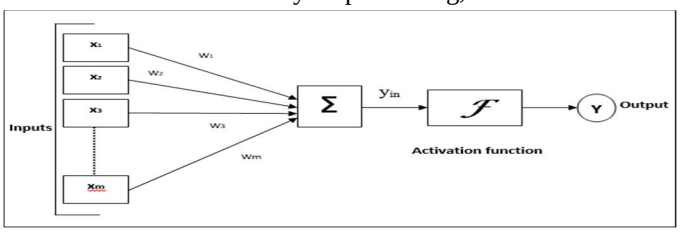

Fig (10): Mathematical model of ANN

For the above general model of artificial neural network, the net input can be calculated as follows,

$$Yin=X1.W1+X2.W2+X3.W3\ldots Xm.Wm \quad (24)$$

i.e., Net input $Yin=\sum_i^m Xi.Wi$

The output can be calculated by applying the activation function over the net input.

$$Y=F(Yin) \quad (25)$$

A mathematical or computer model based on the structure and function of biological neural networks is known as an Artificial Neural Network (ANN). These networks are used to approximate or estimate functions and can work with a large number of unknown inputs. The gradient output will be determined using the hypothesis that has been generated. The outcome of the computed network is explained as follows:

Output of the node of hidden layer:

$$y_j = f(\sum_i w_{ji} x_i - \theta_j) = f(net_j) \quad (26)$$

where, $net_j = \sum_i w_{ji} x_i - \theta_j$

Computational output of the output node:

$$z_l = f(\sum_i v_{lj} y_j - \theta_l) = f(net_l) \quad (27)$$

where, $net_l = \sum_i v_{lj} y_j - \theta_l$

Error of the output node:

$$E = \frac{1}{2}\sum_i (ti - Zi)^2 = \frac{1}{2}\sum_i (ti - f(\sum_i V1j - \theta i))\ ^2 \quad (28)$$

Hypothesis:

$$h_\theta = \theta^T x = \sum_{i=o}^n \theta i x i \quad (29)$$

Gradient update:

$$\theta_j = \theta_j - \alpha \frac{1}{m}\sum_{i=1}^m (h_\theta(x^i) - y^i)\, x_j^i \quad (30)$$

Where, ix = input node, jy = node of the hidden layer, lz = node of output layer, wji = weight value of network between the input node and node of hidden layer, ljv = weight value of network between the nodes of hidden layer and output layer, lt = expected value of the output node, α = learning rate, m = total sample, θ = weight. The ANN's training process is represented in Fig. 11.

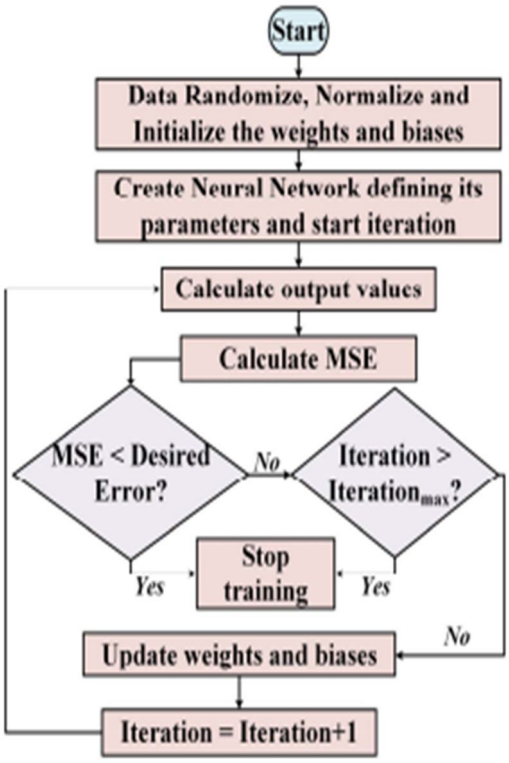

Fig (11): ANN controller training methodology

ISSN: 2321-9653; IC Value: 45.98; SJ Impact Factor: 7.538
Volume 9 Issue XII Dec 2021- Available at www.ijraset.com

III. PROPOSED SYSTEM IN SIMULINK

The Photovoltaic plant and the Wind Turbine Generator (WTG) are connected to the same Point of Common Coupling (PCC) with a sensitive load and are connected to the grid in this system. A DFIG generator is linked to the network through a step-up transformer in the WTG. As illustrated in fig.12, the PV system is linked to the PCC via a single-stage energy conversion (DC-AC inverter) and step-up transformer.

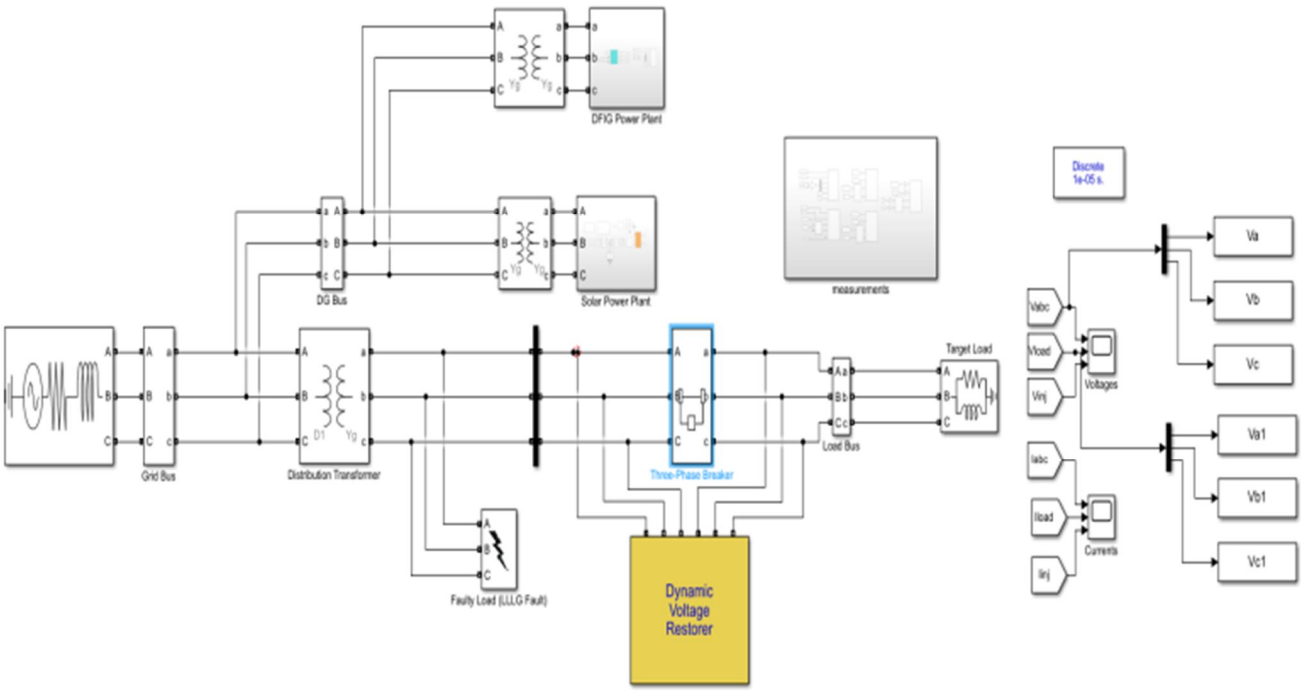

Fig (12): Final SIMULINK Model of Hybrid Distributed Generation System (HDGS) with ANN based DVR

The next stage in the ANN design process is to import this control dataset into the MATLAB ANN design tools. However, it requires careful coding for data separation and transmission to ANN instructions, as well as the selection of the ANN's size. In this project, a 2-layered Feed-Forward ANN is sufficient for this control problem after several iterations. ANN simulink model is generated when control traning process is done with the help of matlab code as shown in fig 13,

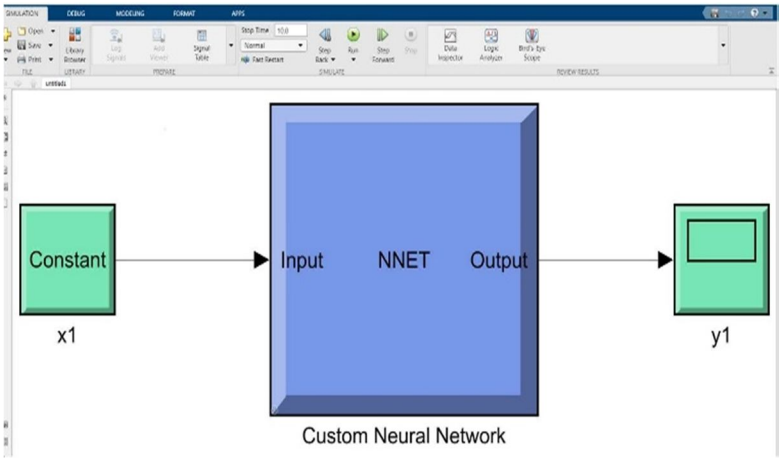

Fig (13): Generated ANN Simulink Block

The objective of this project is to reduce the voltage sag in the load voltage profile caused by short circuit faults in the system. The control method is based on the ANN control approach and includes a DVR series compensation device.

ISSN: 2321-9653; IC Value: 45.98; SJ Impact Factor: 7.538
Volume 9 Issue XII Dec 2021- Available at www.ijraset.com

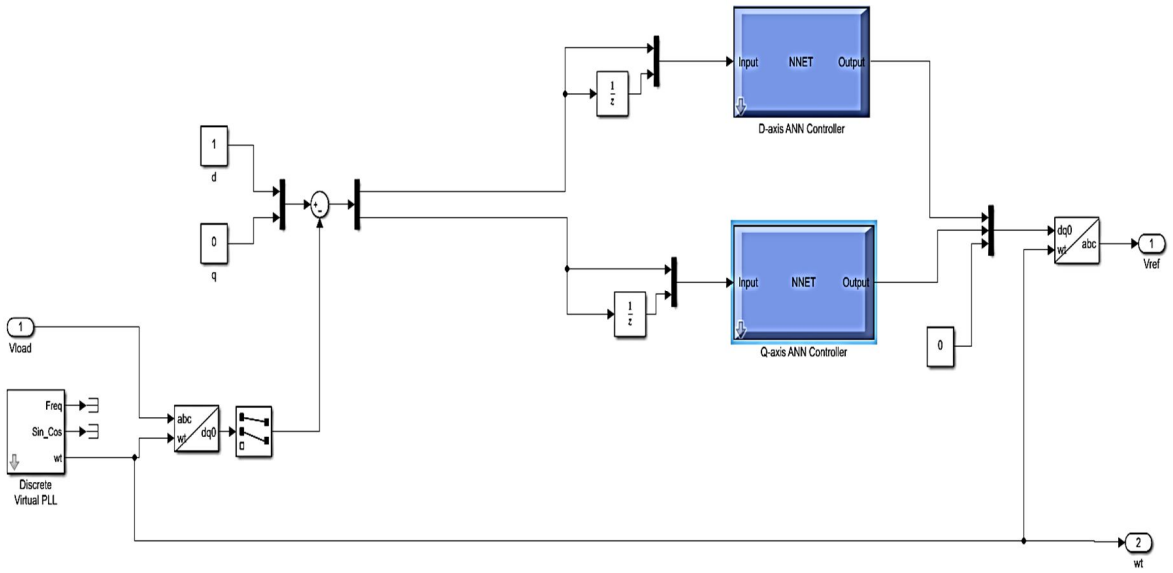

Fig (14): Simulink model of ANN controller for DVR

Fig. 14 shows the final SIMULINK model ANN DVR cobtroller and Fig. 15 represents the Final DVR compensator scheme for mitigating voltage sag caused by a short circuit faults at the load.

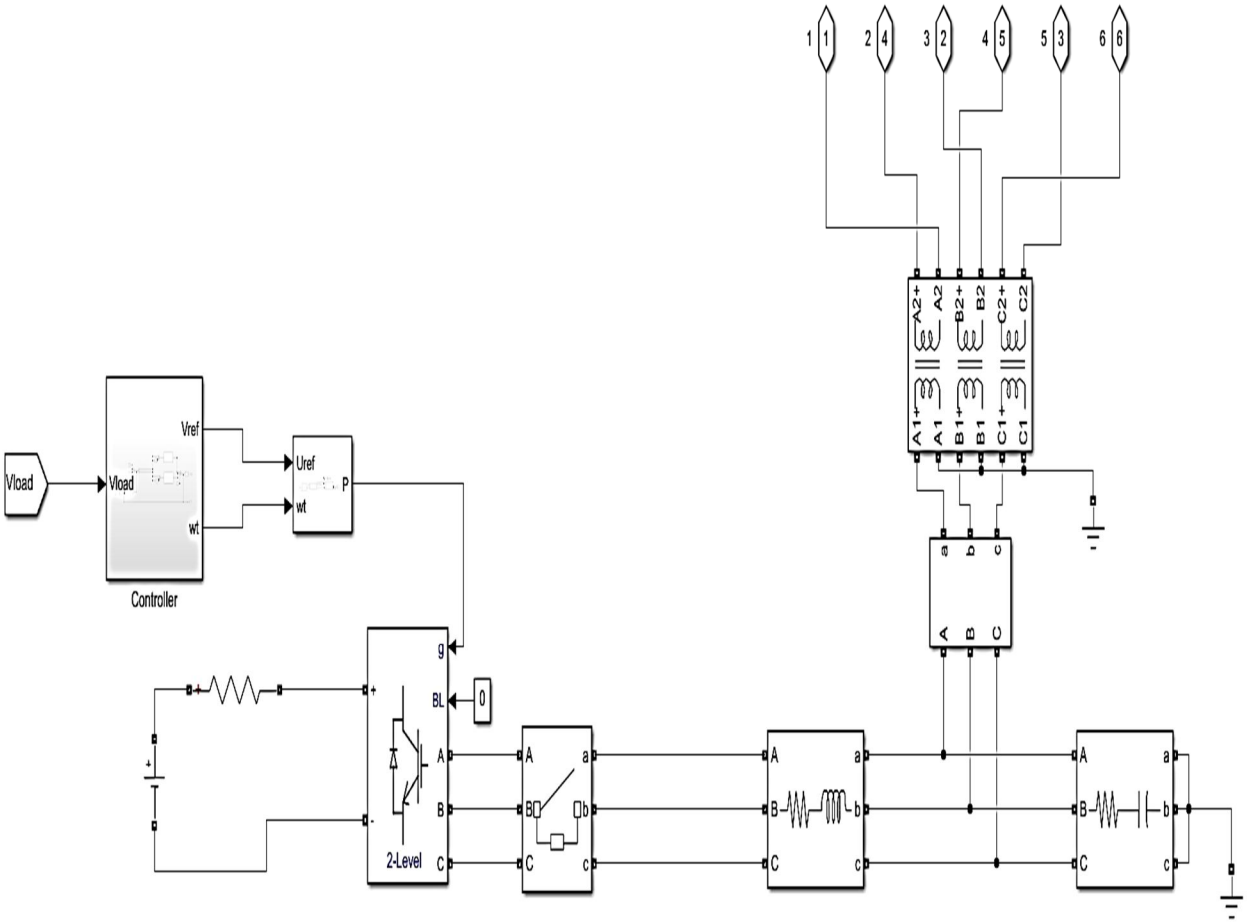

Fig (15): Simulink model of ANN controller based-DVR

The Final parameters of the proposed Simulink power system is tabulated in Table (1).

Table (1): Final SIMULINK Parameters

Parameters		Value
MV grid	Nominal grid L-L voltage	11kV
	Frequency	50Hz
DVR	Inverter filter inductance	0.75mH
	Inverter filter capacitance	10μF
	Dc supply voltage	700V
DFIG	Nominal power	151kw
	frequency	50Hz
	Nominal L-L	575V
Photovoltaic	Plant capacity	106.5kW
	V_{DC}	725V
	Parallel Strings	20
	Series modules	25
Step-up Transformer	Nominal power	1MVA
	Primary voltage	0.4kV
	Secondary voltage	11kV

IV. SIMULATION RESULTS & DISCUSSIONS

The PV array model is scaled to include 25 series modules and 20 parallel strings in order to deliver 106.5KW at an irradiance of 1000W/m² and a DC voltage of *Vdc* = 725V Idc= 147A applied to the Single Stage Converter. The PV array voltage and current are represented in Fig. 17.

PV module is connected to single stage 2-level 3-phase Inverter connected to grid via step-up transformer which results in Phase rms values of voltage and current are 240V and 148A as shown in Fig. 18.

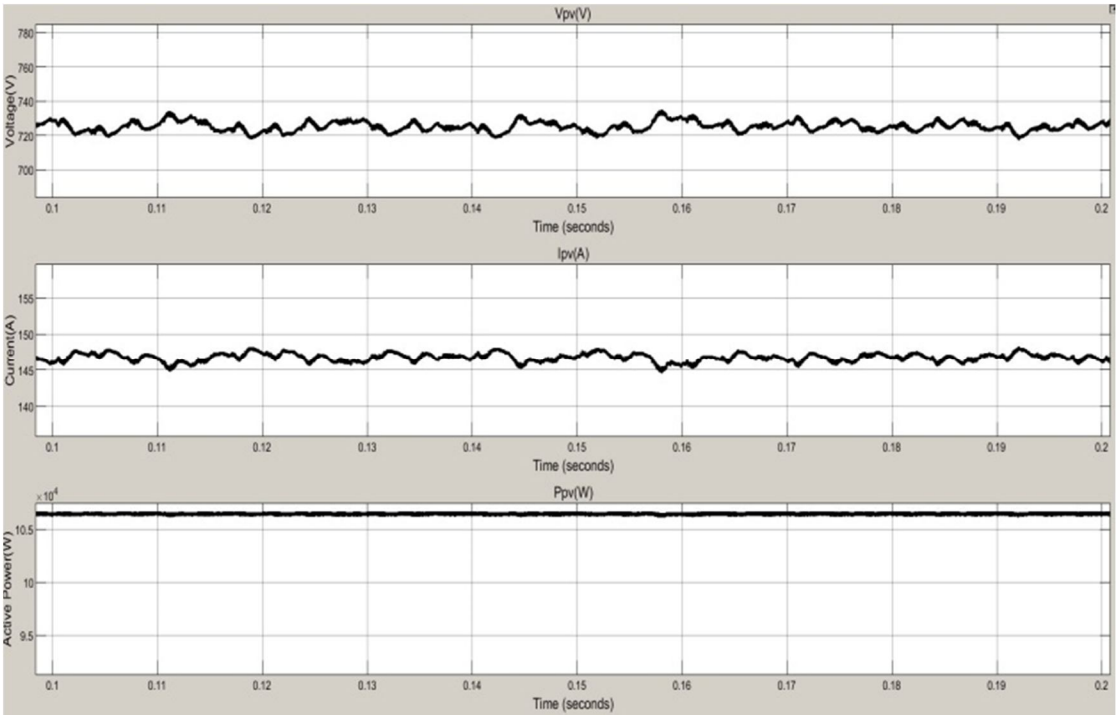

Fig (17): Simulation Results of PV array

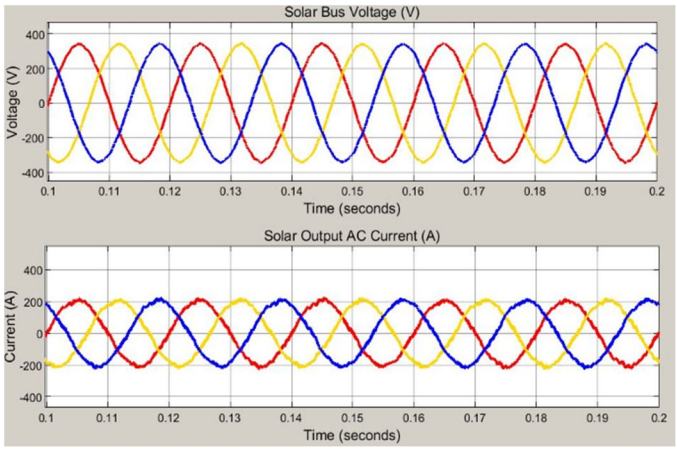

Fig (18): Filtered voltage and current waveforms of PV system

From Fig. 19 it is observed that the 3-phase active and reactive powers are 106.5KW and 133.7VAr respectively.

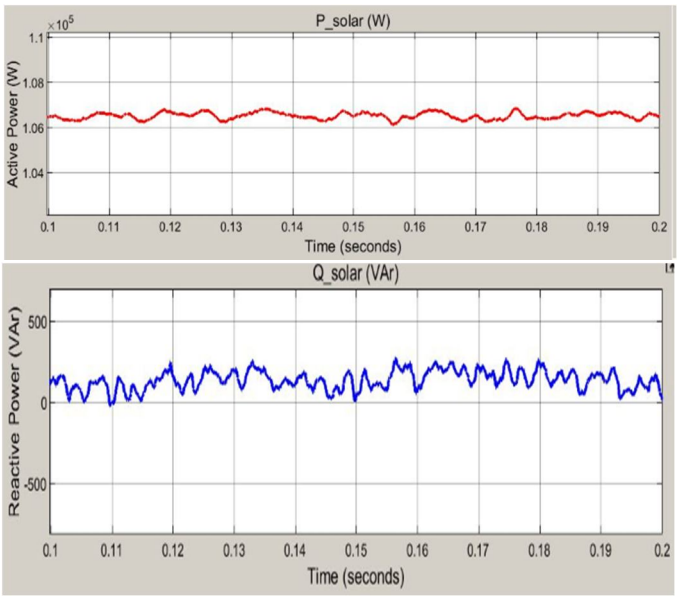

Fig (19): Active and Reactive powers of PV plant

From the Fig.20, it is observed that the DC link voltage value is staggering close to 725V.

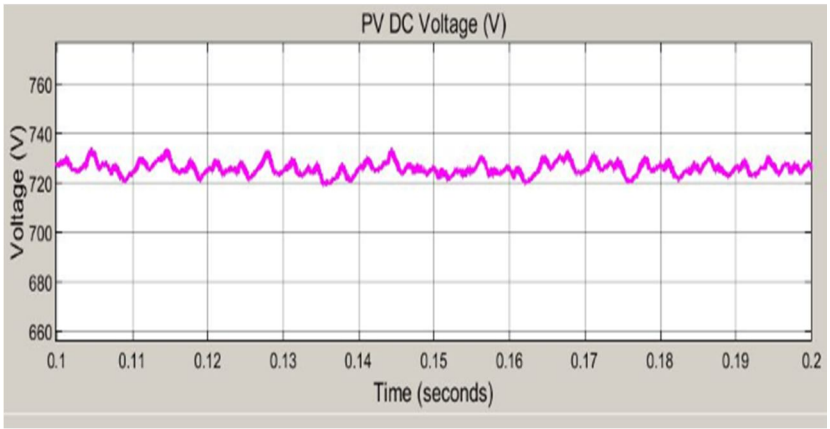

Fig (20): Final Dc link voltage at PV inverter

The final results of DFIG based Wind power plant when 12m/s wind input given to turbine for 5 sec simulation time are visualized by scopes at grid side &rotor side which are discussed in Fig. 21 to 23.

In fig. 21, the DFIG stator voltage, current, active power, reactive power, DC bus voltage and rotor speed (pu) waveforms zoomed at t=4 to 5 seconds are presented. The generated line voltage value is 575V i.e., RMS phase value is 575/1.732 = 332V, RMS phase value of current is 169A. The mean values of 3-phase active and reactive powers are 152.5KW and 70KVAr respectively as shown below fig 22.

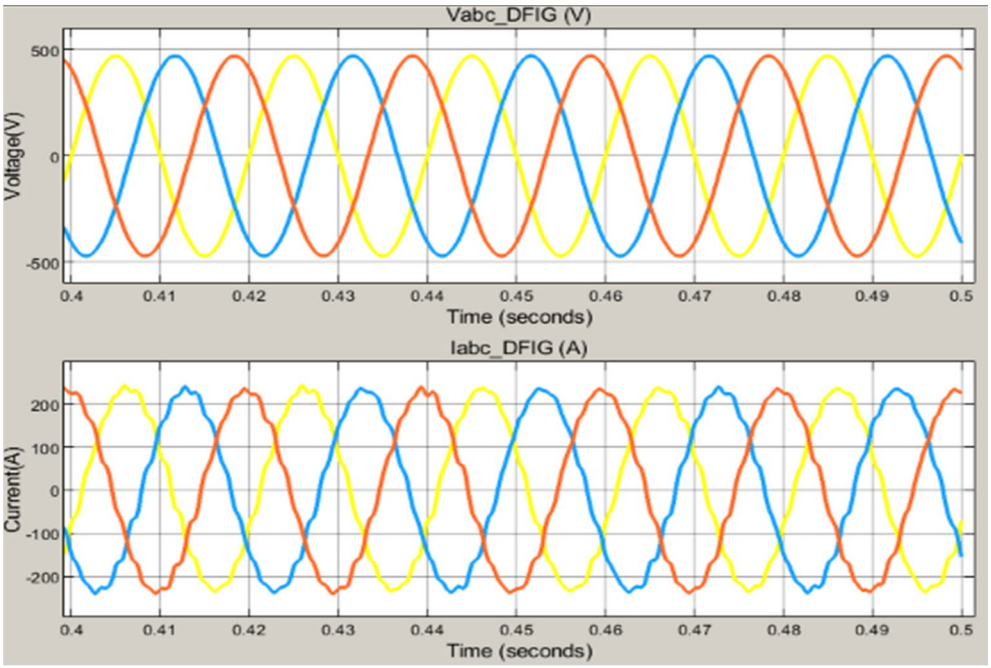

Fig (21): Voltage and current waveforms of DFIG

.

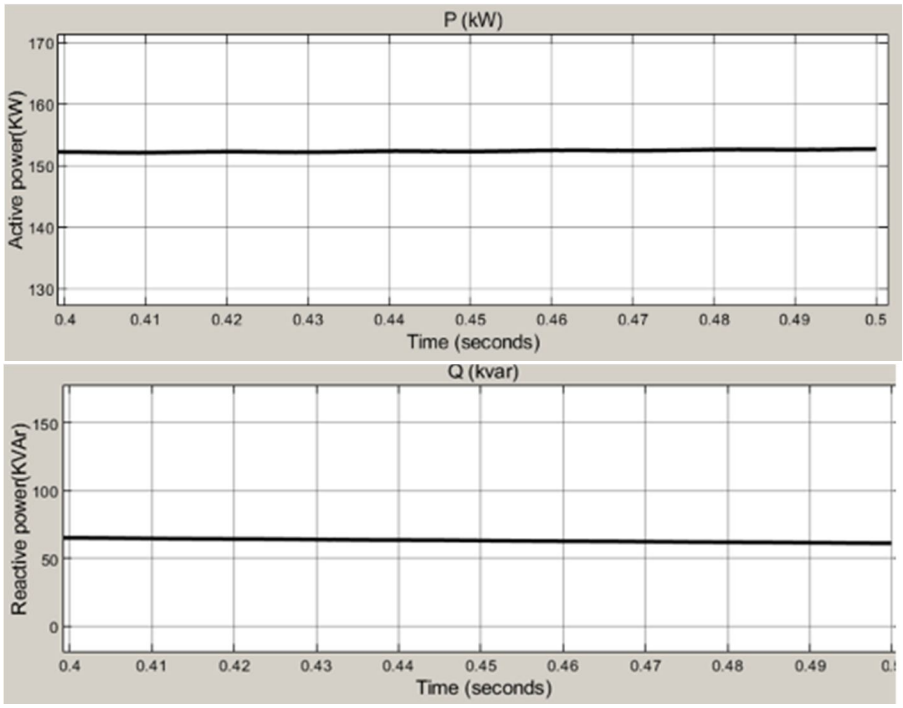

Fig (22): Active and Reactive powers of DFIG

The DC link voltage value is 1150V and turbine rotor speed is 1.23 (pu) as shown in fig 23.

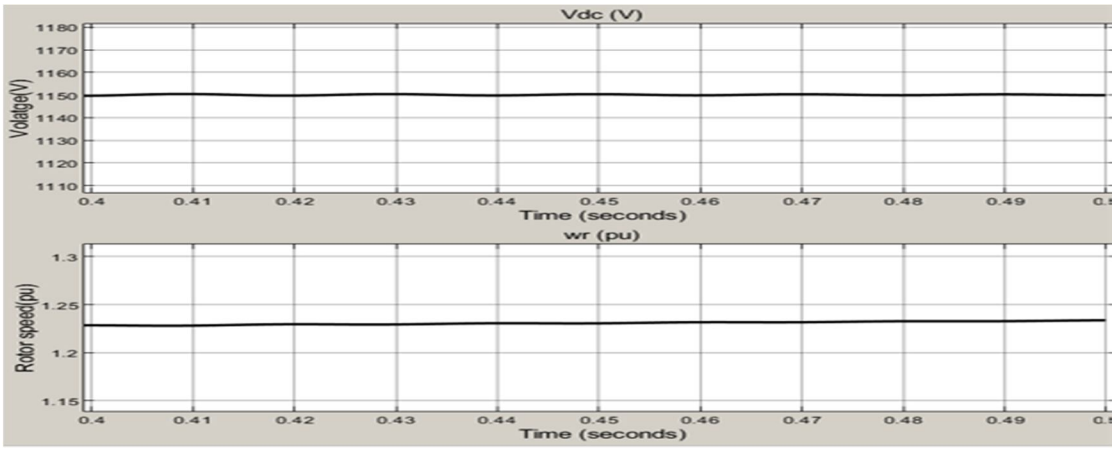

Fig (23): DC link voltage at WTG inverter and Rotor speed (pu)

In fig 24, The final waveforms of voltage, current, active and reactive powers of grid are zoomed at t=0.9 to 1 sec are presented. The grid RMS line voltage value is 11KV and RMS phase value is 11000/1.732=6.351KV and grid RMS phase current value is 7.053A. 3-phase active power consumed value is 111.65KW and 3-phase reactive power supplied value is 70KVAr as shown in fig 25.

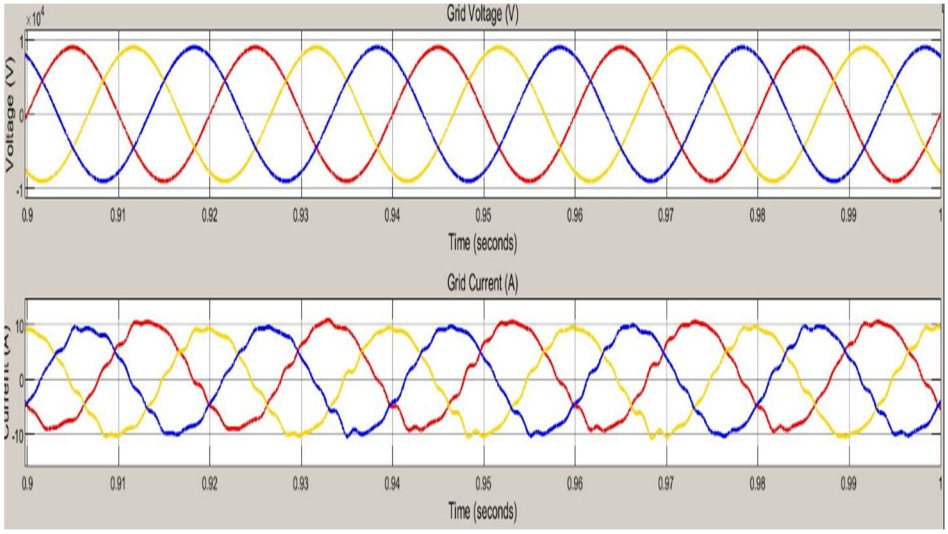

Fig (24): Voltage and Current waveforms of 11kV equivalent grid

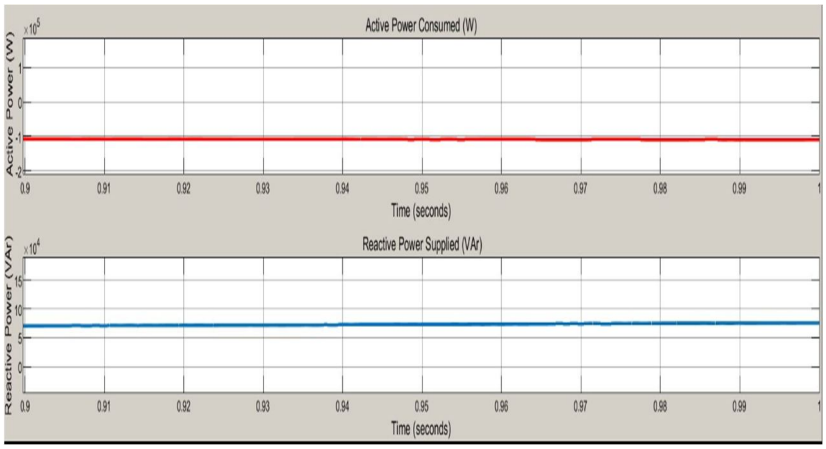

Fig (25): active and reactive powers of 11kV equivalent grid

The final waveforms of voltage, current, active power, reactive power of load shown in Fig (26) after integrating PV-wind systems connected to grid at PCC (Point of Common Coupling) and distribution transformer used to reduce the voltage i.e 400V from 11KV for Industrial load. These waveforms are zoomed at t=0.9 to 1 sec are presented. The load RMS line voltage value is 400, RMS phase value is 400/1.732=230.9V and load RMS phase current value is 272.5A

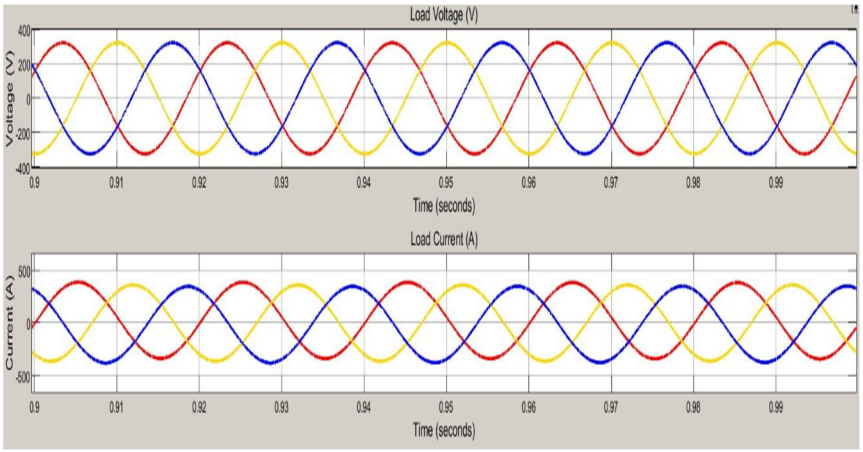

Fig (26): voltage and current of industrial load

The 3-phase active power consumed value is 146.1KW and reactive power consumed value is 97.18KVAr for given rated active and reactive powers are 150KW and 100KVAr as shown in fig 27.

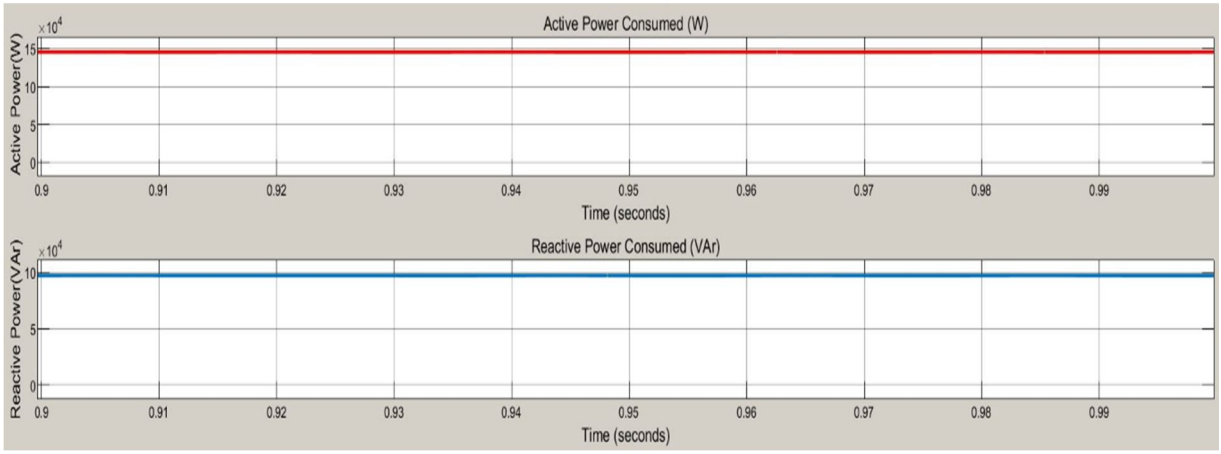

Fig (27): active and reactive powers of industrial load

The common short circuit fault is LG fault applied near to load center of fault period t=0.23 to 0.27 seconds which results in voltage of critical load is shown in Fig. 28.

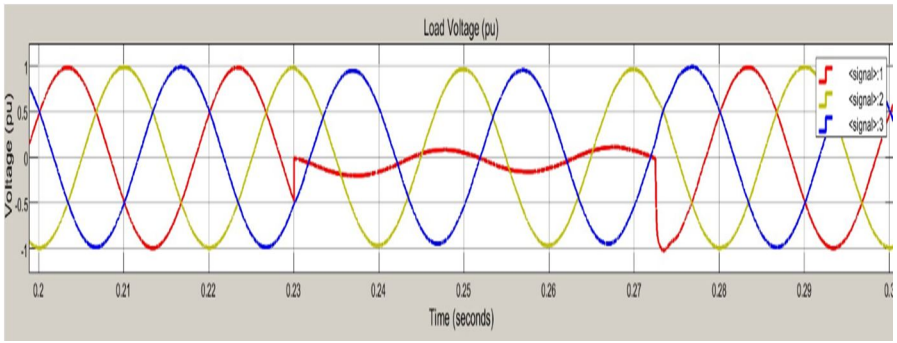

Fig (28): L-G sagged 3-phase load voltage

Voltage Harmonics at load side due to short circuit fault are studied with the help of FFT analysis as shown in fig 29.

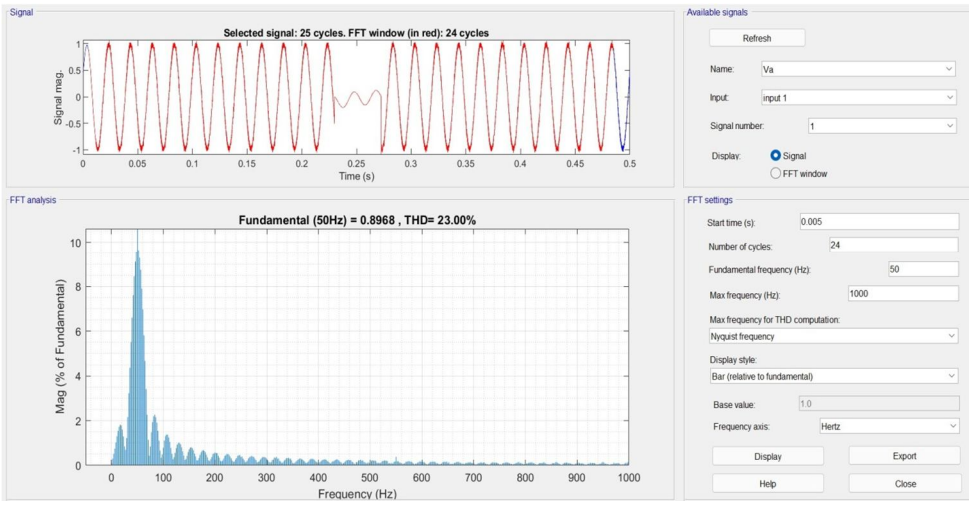

Fig (29): FFT analysis (without compensation)/L-G fault

FFT analysis shows Total Harmonic Distortion (THD) of load phase voltage (Va) in Percentage over maximum number of cycles as shown in Fig 29, THD is 23.00%.

The Final results of voltage sags caused by LG short circuit fault is mitigated by using advanced control technique (ANN) based DVR at load as shown in fig 30.

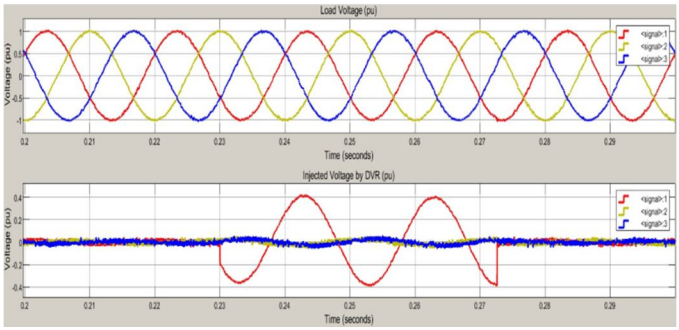

Fig (30): Compensated voltage waveform after DVR application

The voltage Harmonics are caused by short circuit fault (LG) which are suppressed by DVR, studied with the help of FFT analysis as shown in figure 31.

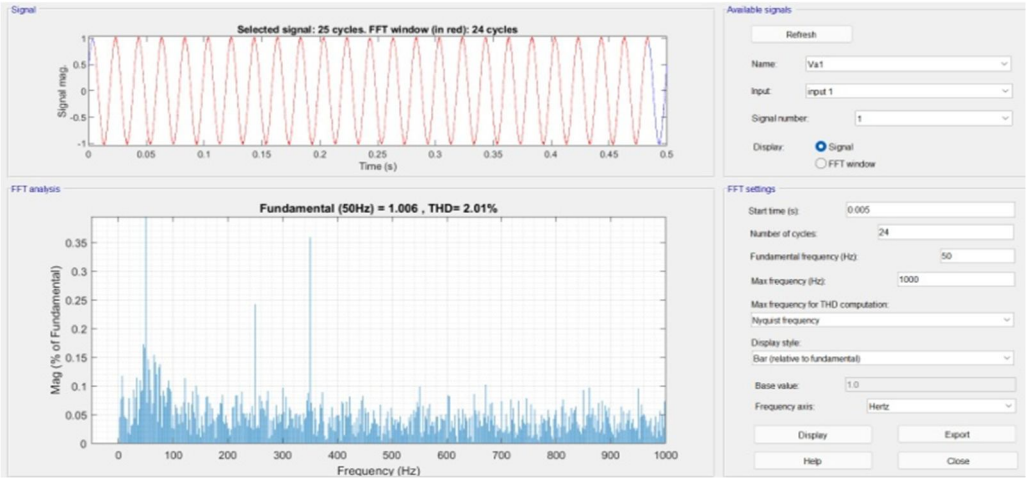

Fig (31): FFT analysis (with DVR compensation)/L-G fault

FFT analysis shows Total Harmonic Distortion (THD) of load phase voltage (Va) in Percentage over maximum number of cycles as shown in Fig31, THD is 2.01%.

The line to line (LL) short circuit fault is applied near to load center of fault period t=0.23 to 0.27 seconds which results in voltage of critical load is show in Fig. 32. The voltage Harmonics at load side due to short circuit fault are studied with the help of FFT analysis as shown in fig 33.

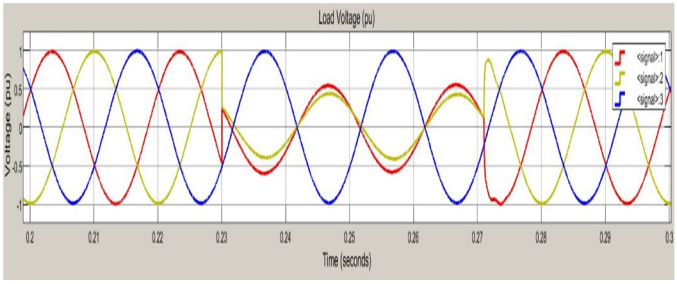

Fig (32): LL sagged 3-phase load voltage

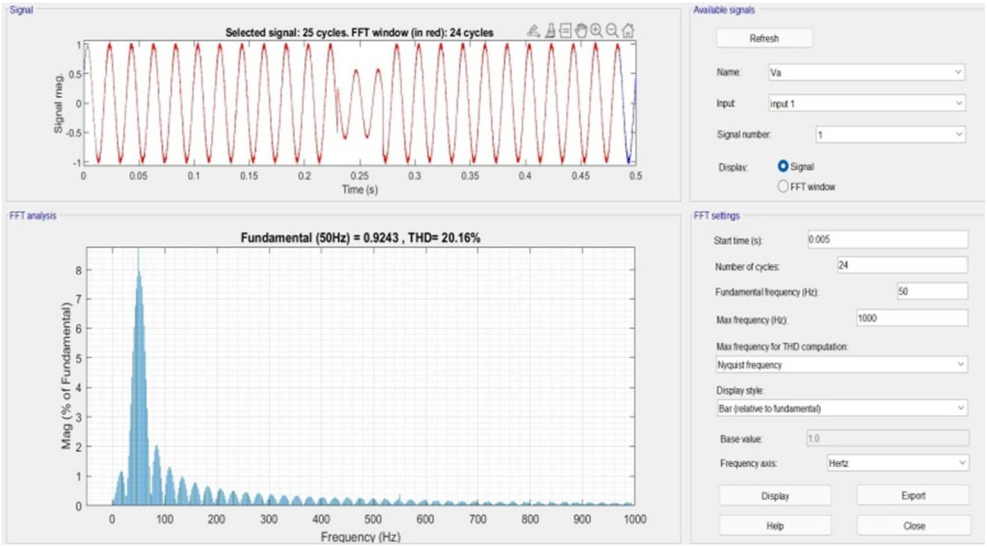

Fig (33): FFT analysis of load phase voltage Va (without compensation)/LL fault

The FFT analysis shows Total Harmonic Distortion (THD) of load phase voltage (Va) in Percentage over maximum number of cycles as shown in Fig 33, THD is 20.16%. The final results of voltage sags caused by LL short circuit fault is mitigated by using advanced control technique (ANN) based DVR at load as shown in fig 34.

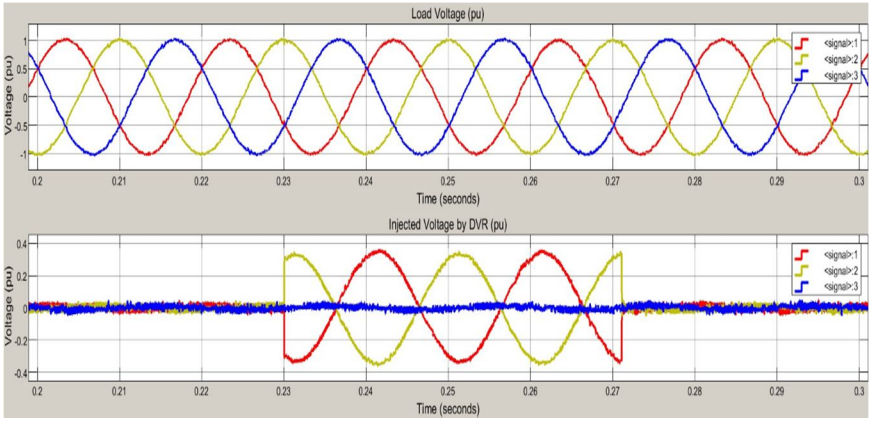

Fig (34): Compensated voltage waveform after DVR application

The Voltage Harmonics are caused by short circuit fault (LL) which are suppressed by DVR, studied with the help of FFT analysis as shown in fig 35.

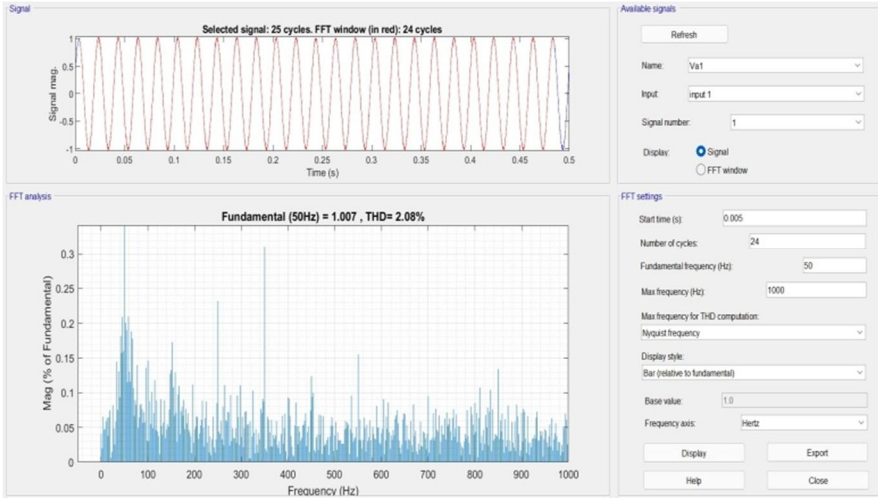

Fig (35): FFT analysis of load phase voltage Va1 (with compensation)/LL fault

The FFT analysis shows Total Harmonic Distortion (THD) of load phase voltage (Va1) in percentage over maximum number of cycles as shown in Fig 35, THD is 2.08%.

The 3-phase short circuit fault (LLL) is applied near to load center of fault period t=0.23 to 0.27 seconds which results of critical load is represented in Fig. 36.

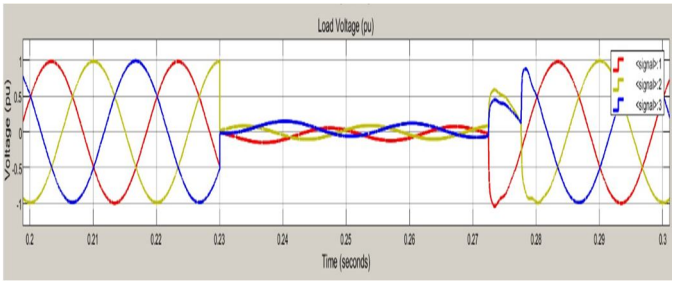

Fig (36): LLL sagged 3-phase load voltage

The voltage Harmonics at load side due to 3-phase short circuit fault (LLL) are studied with the help of FFT analysis for phase 'A' is as shown in fig 37. The FFT analysis shows that the THD of load phase voltage (Va) without compensation in percentage over maximum number of cycles as shown in Fig 37, THD is 23.10%.

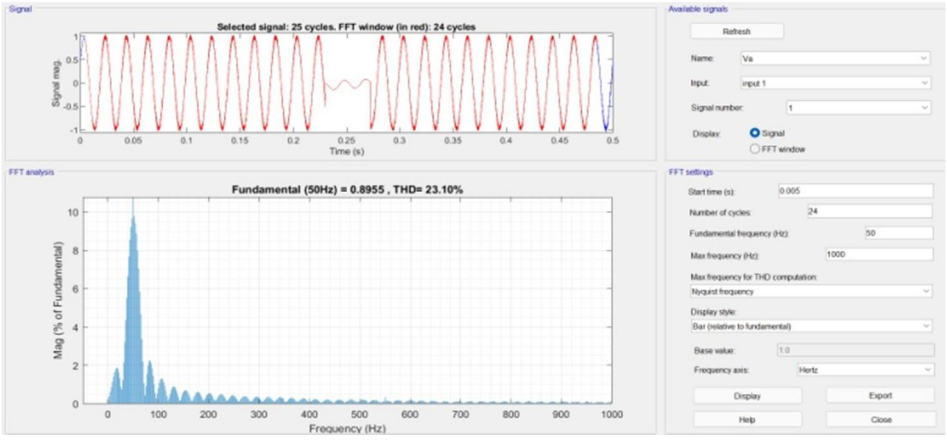

Fig (37): FFT analysis of load phase voltage Va (without compensation)/LLL fault

The final results of mitigation of voltage sags caused by LLL short circuit using ANN based DVR near load centre is as shown in fig 38,

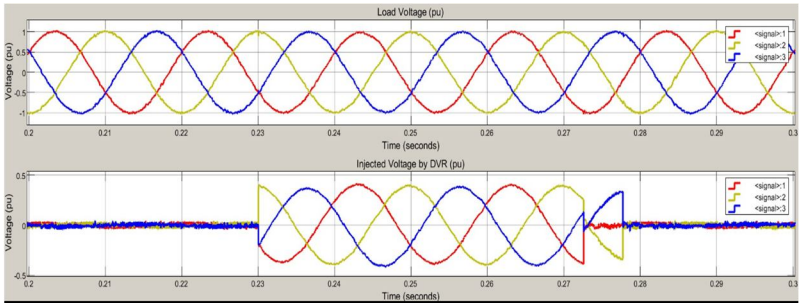

Fig (38): Compensated voltage waveform after DVR Application

The voltage Harmonics are caused by 3-phase short circuit fault (LLL) which are suppressed by ANN-DVR, studied with the help of FFT analysis as shown in fig 39.

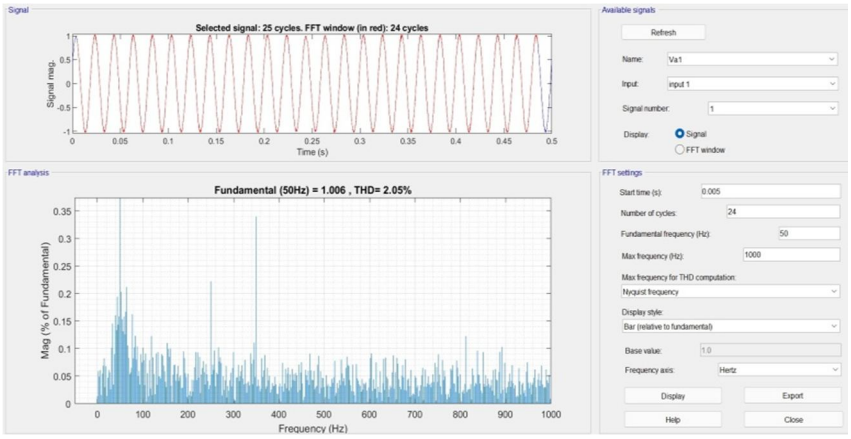

Fig (39): FFT analysis of load phase voltage Va1 (with compensation)/LLL fault

FFT analysis shows Total Harmonic Distortion (THD) of load phase voltage (Va1) in Percentage over maximum number of cycles as shown in Fig 39, THD is 2.05%. The Final waveforms of voltage, current, active power and reactive power at critical load with compensation using DVR as shown in fig 40.

The DVR can readily manage both balanced and unbalanced circumstances, injecting the required voltage components to quickly rectify the supply voltage and keep the load voltage constant. Finally voltage, current, active, and reactive powers are balanced at nominal values, resulting in better distribution network power quality as shown in the fig 40.

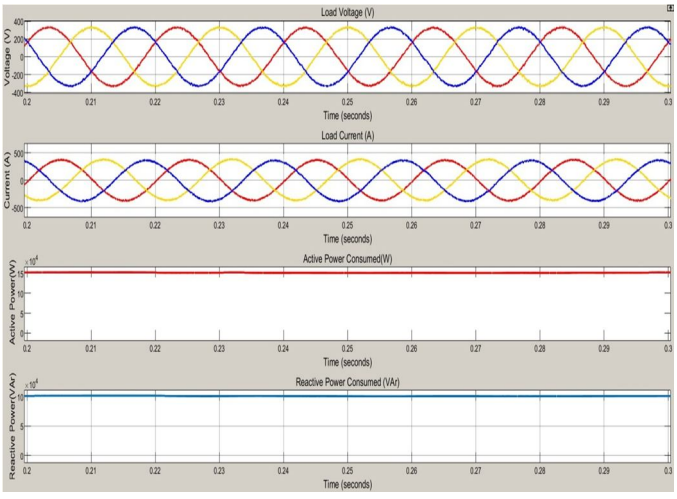

Fig (40): Final Waveforms of sensitive load with compensation using DVR

Table (2): THD % of Various faults with and without Compensation

TYPE OF FAULTS	TOTAL HARMONIC DISTORTION (THD %)	
	WITHOUT COMPENSATION (DVR OFF)	WITH COMPENSATION (DVR ON)
LG	23% (Va)	2.01% (Va1)
LL	20.16% (Va)	2.08% (Va1)
LLG	24.09% (Va)	2.06% (Va1)
LLL	23.10% (Va)	2.05% (Va1)
LLLG	23.10% (Va)	2.10% (Va1)

V. CONCLUSION

The proposed configuration focuses on building an intelligently controlled DVR to protect an industrial load adjacent to Hybrid Distributed Generation. In order to model the power quality issues (like voltage sag, harmonics, poor power factor etc.,) in the grid supply, I have implemented a Grid-Connected PV system integrated to a DFIG based wind power plant. The consequence of integrating a substantial proportion of distributed generation and various short circuit faults near target load has resulted in voltage sag and harmonics. A simulation study thus carried out to demonstrate the effectiveness of the proposed ANN-DVR control system to improve the FRT capability of the Industrial load under different fault scenarios. This control strategy resulted in faster voltage restoration with high harmonics suppression capabilities. Simulation results showing the DVR performance during voltage sag have been presented. Comparison of the proposed method with the popular PI controller has been carried out, where the proposed ANN controller appeared as the best option to restore system voltage while mitigating THD to the greatest extent (THD<2.5%).

Thus, the proposed DVR protects the target load from grid side altercations caused by harmonics generated by DGs and short circuit faults close to the load centre, allows for rapid voltage recovery and reduces power oscillation overshoot in accordance with FRT requirements.

REFERENCES

[1] Arundhati R. Karkhanis, " Integration of PV and DVR Systems for Overcoming Unbalance of System during Critical Loads," IJIRSET, vol.5, Issue 5, May 2016, DOI:10.15680/IJIRSET.2015.0506067.

[2] Mohamed Shaaban, Christy E. A. Benedict, "Effect of Distributed Wind Generation on the Voltage Sag of Distribution Networks," IJRTE, Volume-8, Issue-4, November 2019, DOI:10.35940/IJRTE.118419.

[3] H. Laabidi and A. Mami, "Grid connected Wind-Photovoltaic hybrid system," in 2015 5th International Youth Conference on Energy (IYCE), pp. 1-8,2015.

[4] X. Liang, "Emerging power quality challenges due to integration of renewable energy sources," IEEE Transactions on Industry Applications, vol. 53, pp.855-866, 2017.

[5] Omar Noureldeen, Ahmed M. A. Ibrahim," Modeling, Implementation And Performance Analysis of a Grid-Connected Photovoltaic/Wind Hybrid Power System" International Conference on Innovative Trends in Computer Engineering (ITCE),2018. Deepa

[6] Francis and Tomson Thomas, "Mitigation of Voltage Sag and Swell Using Dynamic Voltage Restorer" 2014 Annual International Conference on Emerging Research Areas: Magnetics, Machines and Drives (AICERA/iCMMD), 2014, pp. 1-6.

[7] Shazma Khan, Balvinder Singh and Prachi Makhija, "A Review on Power Quality Problems and its Improvement Techniques" 2016 International Conference on Advances in Electrical, Electronic and System Engineering, 14-16 November 2016, Putrajaya, Malaysia.

[8] Lucas F. J. Meloni, Angelo.J.J.Rezek and Enio.R.Ribeiro, "Small-Signal Modeling of a Single-Phase DVR for Voltage Sag Mitigation"17th International Conference on Harmonics and Quality of Power (ICHQP), 2016, pp. 55-59.

[9] BLS Shraddha, Sonicka R, "Simulation and Analysis of Dynamic Voltage Restorer," 3rd IEEE International Conference on Recent Trends in Electronics, Information & Communication Technology (RTEICT-2018), MAY 18th &19th 2018.

[10] Samprati Mohanty, Bibhu Prasad Ganthia, "Compensation of Voltage Sag Using DVR with PI controller," International Conference on Electrical, Electronics, and Optimization Techniques (ICEEOT) – 2016.

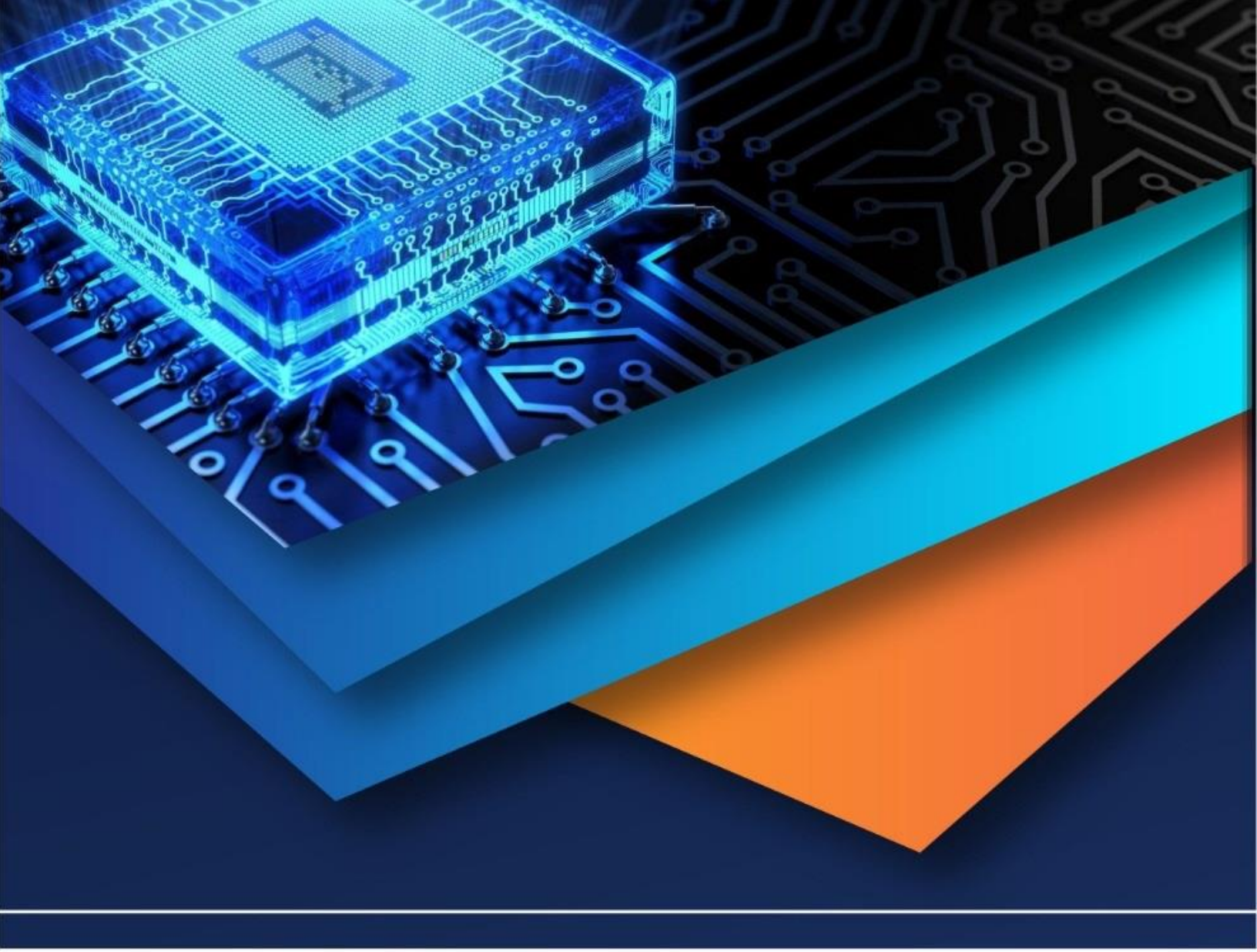

10.22214/IJRASET

45.98

IMPACT FACTOR: 7.129

IMPACT FACTOR: 7.429

INTERNATIONAL JOURNAL FOR RESEARCH

IN APPLIED SCIENCE & ENGINEERING TECHNOLOGY